tapraid5/z3t-mrm/z3t-mrm/z3t00904/z3t1813d04g | sweigarm | S=5 | 6/29/04 | 6:07 | Art: 104-6832

Magnetic Resonance in Medicine 52:000–000 (2004)

Ultrafast 2D NMR Spectroscopy Using Sinusoidal Gradients: Principles and Ex Vivo Brain Investigations

Noa Sela,[1] Hadassa Degani,[1] and Lucio Frydman[2*]

A new methodology capable of delivering complete 2D NMR spectra within a single scan was recently introduced. The resulting potential gain in time resolution could open new opportunities for in vivo spectroscopy, provided that the technical demands of the methodology are satisfied by the corresponding hardware. Foremost among these demands are the relatively short switching times expected from the applied gradient-echo trains. These rapid transitions may be particularly difficult to accomplish on imaging systems. As a step toward solving this problem, we assessed the possibility of replacing the square-wave gradient train currently used during the course of the acquisition by a shaped sinusoidal gradient. Examples of the implementation of this protocol are given, and successful ultrafast acquisitions of 2D NMR spectra with suitable spectral widths on a microimaging probe (for both phantom solutions and ex vivo mouse brains) are demonstrated. Magn Reson Med 52:000–000, 2004. © 2004 Wiley-Liss, Inc.

Key words: ultrafast 2D NMR; magnetic resonance spectroscopy; brain metabolites; 2D TOCSY spectra; sinusoidal gradients

NMR spectroscopy has become an increasingly common tool in the investigation of both normal function and disease in living systems (1–3). Two-dimensional (2D) NMR, in particular, offers two distinct advantages over its simpler one-dimensional (1D) spectroscopic counterparts: enhanced resolution as resonances are spread over a plane rather than along a single frequency dimension, and spectral assignment opportunities stemming from correlations between pairs of related resonances. In recent years, several studies have utilized 2D NMR in order to investigate, within whole-body magnetic resonance imaging (MRI) settings, in vivo metabolism and function (4–11). Most of these studies focused on brain investigations at varying degrees of localization (5–10), while others introduced 2D NMR as a promising tool for breast and prostate cancer analysis (11,12). Although 2D NMR methods are potentially useful for in vivo investigations, the routine clinical use of such techniques is hampered by the relatively lengthy nature of the procedure involved. Long acquisition times also deprive 2D NMR from much of the temporal resolution required to efficiently follow dynamic metabolite changes. 2D spectroscopy inherently takes longer to perform than 1D NMR approaches, since it necessitates the monitoring of correlations among pairs of spin evolution frequencies. To implement such correlations, 2D NMR relies on a scan-by-scan incrementation of a time variable t_1 encoding the indirect-domain interactions Ω_1 (13). Since each t_1 increment corresponds in essence to an independent 1D NMR experiment, long acquisition times become inherent even for systems that possess abundant signal-to-noise ratios (SNRs). A number of proposals have recently been made to alleviate this extended acquisition-time problem (14), including an "ultrafast" approach capable of affording complete 2D NMR spectra within a single scan (15–17). Because it offers shorter acquisition times, this new protocol could assist investigators in developing new applications for 2D in vivo MR spectroscopy (MRS). In this study we discuss the challenges we encountered when we attempted to import this technique into a small imaging system, as well as some of the solutions we accordingly devised.

THEORY

Ultrafast 2D NMR Acquisitions Using Sinusoidal Gradients

The principles of single-scan 2D NMR have been discussed elsewhere (15–17), and hence we shall only briefly mention them here in connection with the application of specific modifications. Figure 1 illustrates a generic sequence capable of affording 2D NMR spectra within a single scan, assuming for simplicity that the spatial encoding it requires was achieved by applying a train of N_1 spatially-selective radiofrequency (RF) pulses. Spins excited by such an RF pulse train will undergo a sequential excitation, and thus accumulate an overall internal evolution phase ϕ that depends on their respective evolution times t_1. Since the application of a field gradient makes these indirect evolution times proportional to the spins' spatial positions z_j within the sample, the spatially-selective spin evolution phases can be written as, $\phi(z_j) = e^{iC\Omega_1(z_j - z_{N_1})}$ where $C = 2T_p G_e / |O_i - O_{i+1}|$ is a spatiotemporal ratio, and Ω_1 is the internal spin interaction we are attempting to measure. Following the mixing period, a gradient G_a is applied in conjunction with the signal digitization. This gradient has the ability to "unwind" the spiral of $\{\phi_j(z_j)\}_{j=1,N_1}$ magnetizations created over the evolution period, leading to observable echoes whenever $k = \gamma_a \int_0^t G_a(t')dt' = -C\Omega_1$. This constructive echoing of the spin-packets constitutes the "peaks" observed in ultrafast NMR along the indirect dimension. One can reverse the effective k-decoding simply by reversing the current that generates the field gradient. This allows one to monitor how the phases in the resulting gradient echoes develop as

[1]Department of Biological Regulation, Weizmann Institute of Science, Rehovot, Israel.

[2]Department of Chemical Physics, Weizmann Institute of Science, Rehovot, Israel.

Grant sponsor: NIH; Grant number: CA42238; Grant sponsor: Israeli Science Foundation; Grant number: 296/01; Grant sponsor: Minerva Foundation (Munich, FRG).

*Correspondence to: Professor Lucio Frydman, Department of Chemical Physics, Weizmann Institute of Science, Rehovot 76100, Israel. E-mail: lucio.frydman@weizmann.ac.il

Received 12 January 2004; revised 4 May 2004; accepted 4 May 2004.
DOI 10.1002/mrm.20204
Published online in Wiley InterScience (www.interscience.wiley.com).

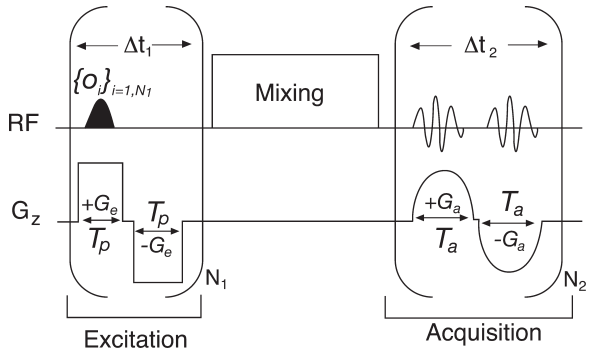

FIG. 1. Generic scheme proposed for incorporating sinusoidal acquisition gradients into single-scan 2D NMR spectroscopy: a train of N_1 frequency-shifted pulses with offsets $\{O_i\}_{1 \geq i \geq N1}$ sequentially excites spins throughout different positions in the sample. Data are then collected under the action of a sinusoidal acquisition gradient $G_a(t) = G_o sin(\pi t/T_a)$, which unravels the corresponding k/ν_1 indirect-domain frequency axis according to $k = [1 - cos(\pi t/T_a)] \cdot \frac{G_o T_a}{\pi}$.

a function of a time t_2. One can thus obtain a complete 2D NMR data set by sorting out the collected data points according to their k and t_2 coordinates, and Fourier transforming the phase-modulated echo peaks along k/ν_1 as a function of their t_2 values.

One of the main complications that arose when we attempted to implement this protocol in an MRI setting resulted from the relatively slow switching time that characterizes gradients in such systems. Whereas modern spectroscopy probe heads usually demand <10 μs to reverse a ~0.5 T/m gradient, the much larger gradient coil diameter associated with imaging setups results in at least an order of magnitude increase in the ensuing switching times. This in turn has strong deleterious effects on the performance of the ultrafast experiment, since long gradient switching times lead to a concomitant increase in the associated dwell times, and thus to a decrease in the spectral window ranges that can be characterized along the direct (and to some extent also the indirect) dimension. A well-known solution for overcoming artifacts related to long gradient switching times consists of shaping the field gradients into sinusoidal functions characterized by lower slew rates (18). A similar strategy could then be used to alleviate requirements in the single-scan 2D NMR protocol. The incorporation of sinusoidal gradients into this kind of experiment can be divided into two different steps: the use of sinusoidal gradients during the spins' excitation, and the use of shaped gradients during the data acquisition. The first of these tasks is far from trivial, and demands that the excitation modality used so far in the spectroscopy be changed. (An account describing current progress in this area will be given elsewhere.) The second option, on the other hand, is fairly straightforward, and yields an immediate improvement in the spectral widths that can be covered. Its implementation and demonstration forms the focus of the present work.

A feature associated with the introduction of sinusoidal gradients is that when these gradients are combined with constant data acquisition rates, they result in unequal intervals in the sampling Δk of the indirect ν_1-domain. This nonlinearity in the sampling of the k-axis is not as severe a hindrance in this kind of experiment as it is, for example, in echo-planar imaging (EPI) (18), where the data must be subjected to Fourier transformation along the k-axis. The only Fourier transform involved in ultrafast 2D NMR occurs along the direct t_2 domain, and this can be implemented in a straightforward manner regardless of the gradient's periodic functionality, since the points' separation along this axis always remains $\sim 2T_a$. In fact, one need only subject the data to an interpolation based on equidistant Δk increments to obtain a conventional spectral display, where adjacent points along the ν_1 axis appear separated by constant increments $\Delta\nu$. We implemented such "regridding" throughout this work using a simple unidimensional linear interpolation whereby a complex data value D at a particular k/ν_1 coordinate was inferred from corresponding data values $D_1 = f(k_1)$, $D_2 = f(k_2)$ measured at nearest-neighbor points by the classical formula $D(k) = \frac{k - k_2}{k_1 - k_2} D_1 + \frac{k - k_1}{k_2 - k_1} D_2$. For the remainder of the data processing, this calculation was carried out with the use of Matlab© 6.5 (The Math Works Inc.) software, specifically with the *interpl* built-in routine. It is also worth remarking that since the k-space trajectory explored by a sinusoidal gradient is $2/\pi$ times smaller than that spanned by a rectangular gradient of the same maximum intensity, the relevant formula for calculating the indirect domain spectral width (15–17) also had to be multiplied by this factor for a proper representation.

MATERIALS AND METHODS

To test the feasibility of implementing ultrafast 2D NMR with sinusoidal gradients, we conducted a series of experiments at 9.4 T on a DMX-400 Bruker® NMR spectrometer equipped with a 40-A microimaging accessory. We used a probe head with sample dimensions of 0.9 cm in length and 1.0 cm in diameter (~0.7 cm^3 voxel size), which was equipped with a proton insert characterized by a 15.2-μs 90° pulse at the maximum attainable RF power. Actively-shielded gradient coils giving up to 2 T/m with 250 μs typical rise times were available in this system. Despite the high gradient fields delivered by this system, we found that substantial distortions appeared in the spectrum when gradients began to exceed ~0.8 T/m, and hence gradients below this value were used.

The ultrafast experiments implemented in this study were of the TOCSY type (13). They were based on the general layout given in Fig. 1, and incorporated the following parameters: $N_1 = 40$ square excitation pulses (each 170 μs long and applied at $\Delta O = 6$ kHz offset increments while in the presence of $G_e = 0.6$ T/m), data acquisition with $N_2 = 128$, $T_a = 305$ μs, $G_o = 0.6$ T/m, and dwell time = 5 μs. The mixing consisted of a 40-ms MLEV-16 isotropic sequence encompassing a train of 180° pulses, each 120 μs long. When implemented in aqueous solutions, the pulse sequence was preceded by some form of water suppression (either a long (1 s) presaturation pulse, or a chemical shift-selective (CHESS) sequence with three 90° Gaussian pulses covering a bandwidth of 300 Hz (the last one with overtipping) followed by 3-ms-long, 1.2-T/m gradient pulses (19)).

tapraid5/z3t-mrm/z3t-mrm/z3t00904/z3t1813d04g | sweigarm | S=5 | 6/29/04 | 6:07 | Art: 104-6832

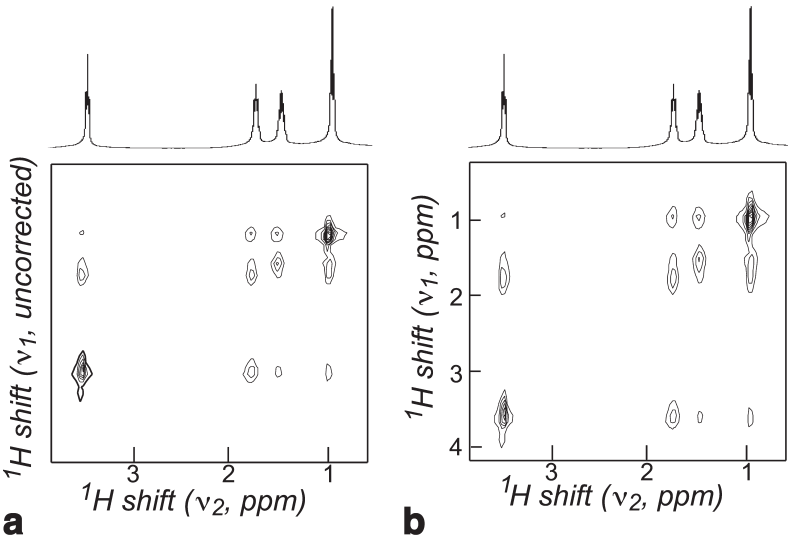

FIG. 2. Comparison between results obtained from an ultrafast 2D TOCSY NMR experiment using sinusoidal gradients on an *n*-butylchloride sample, before (**a**) and after (**b**) the data were subjected to the interpolation procedure described in the text.

Three main samples were tested in this work. Because of its spectral simplicity and lack of solvent background complications, *n*-butylchloride was chosen to both tune the gradient operation and test the proper performance of the postacquisition processing software. In addition, a phantom solution was prepared with a mixture of abundant brain metabolites dissolved in D_2O: 37.5 mM N-acetyl aspartate (NAA), 30 mM creatine (C), 9 mM choline chloride (Ch), 22.5 mM myo-Inositol (mI), 37.5 mM glutamic acid (Glu), and 15 mM lactic acid (Lac), adjusted with NaOH to pH $\approx$ 7. Finally, to test the feasibility of the experiment in an ex vivo tissue specimen, we suspended three dissected brains of SCID mice ($\sim$3 months old) in D_2O and loaded them into the 10-mm NMR tube. In all cases the sample temperature was maintained at 298 K.

RESULTS AND DISCUSSION

The results of single-scan 2D NMR spectroscopy with sinusoidal gradients, as well as the effects introduced by those gradients due to their nonlinear *k*-axis sampling of the 2D NMR data, are illustrated in Fig. 2 for a sample of *n*-butylchloride. Figure 2a presents noninterpolated 2D ^{1}H TOCSY data with peaks along the indirect domain appearing at odd positions, due to the uneven rate at which the sinusoidal gradients scanned the corresponding k/ν_1 axis. As shown in Fig. 2b, a suitable interpolation of the data into a regular grid separated by constant Δk increments can compensate for this distortion. To carry out this data postprocessing, it is important to know the relative timing between the gradients' action and the spectrometer's collection of the data points. For instance, we found that although the sequences had been programmed to begin simultaneously, in all of the 2D pulse sequences written for this study the data acquisition process began $\sim$60 μs in advance of the sinusoidal gradient's activation. Unless it is properly accounted for, this mistiming will result in an incorrect interpolation, and considerable distortions of the spectral line shapes. Apart from this hardware-dependent complication, we found that the sinusoidal gradients did not present any major challenges, and they allowed us to bypass the relatively long switching times of imaging setups.

The potential of the current approach was investigated in a series of brain models. Figure 3 compares 2D TOCSY NMR spectra acquired on a brain phantom sample by means of the ultrafast protocol, as well as the traditional t_1-incremented method. Both sets of results clearly convey similar information, with several common cross-peaks identifiable for various metabolites placed in the phantom. Figure 4 further illustrates this point with an additional series of 2D TOCSY NMR results, this time recorded on ex vivo mouse brain specimens. Since these data were collected from postmortem brains, large contributions from

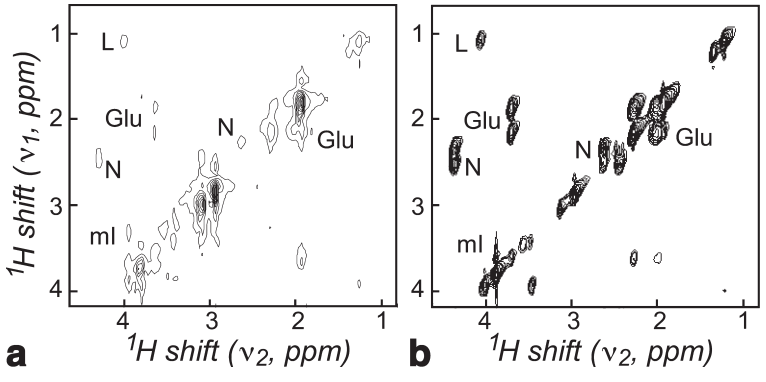

FIG. 3. Comparison between 2D ^{1}H TOCSY NMR spectra collected with the use of the ultrafast (**a**) and conventional (**b**) protocols on a brain phantom sample. The total acquisition time for image **a** was 500 ms. The total acquisition time for image **b**, which involved the collection of 128 phase-cycled t_1 increments and 4K t_2 points, was 23 min 45 s. Shown are cross-peaks assigned to Lac (L), NAA (N), Glu, and mI.

AQ: 10

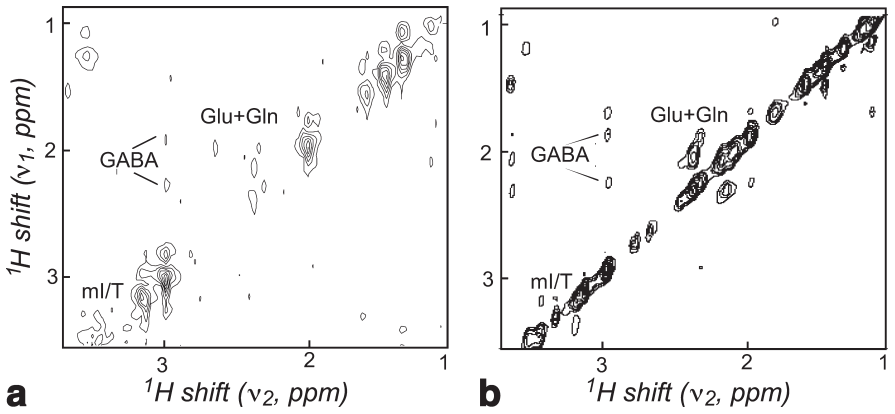

FIG. 4. Idem as in Fig. 3, but with the 2D NMR spectra acquired ex vivo on three brain specimens excised from SCID mice and suspended in deuterated water. Indicated are cross-peaks tentatively assigned to NAA (N), glutamate and glutamine (Glu, Gln), GABA, taurine (T), and mI species.

metabolites that were not present in the synthetic phantom could be seen in the 1D and 2D ^{1}H NMR spectra—particularly in the 1–1.9 ppm region. Aside from these peaks, which became progressively stronger with time, horizontal profiles of selected resonances revealed once again similar cross-peak patterns for both the normal and ultrafast 2D NMR experiments performed on excised brain tissue.

Despite the correspondence revealed by Figs. 3 and 4 between the ultrafast and conventional 2D NMR results, one cannot help but notice the lower quality of the ultrafast counterparts. This drop in quality was also noticed when we utilized the microimaging hardware to implement ultrafast experiments (such as COSY) that were less demanding in terms of RF inhomogeneity. The decrease in quality was only marginally improved by the co-addition of a number of phase-cycled scans, and hence cannot be attributed to limitations in the methodology's sensitivity. Therefore, we are forced to conclude that although sinusoidal acquisition gradients effectively make it possible to overcome the relatively long recovery times of imaging gradient setups, they still leave a number of technical issues to be resolved. We associate these issues mainly to two forms of gradient non-idealities: one involving systematic gradient imbalances throughout the course of the spins' excitation and acquisition processes, and the other to substantial residual eddy currents. As explained elsewhere (16), the first of these artifacts can bring about severe line-shape distortions due to a progressive delaying in the positioning of the k/ν_1 echo peaks. However, these artifacts can be compensated for by either a real-time modification of the applied gradient shapes or, as was done throughout the course of these studies, a post-acquisition shearing of the data. Eddy-current artifacts, by contrast, are harder to compensate for, and have more severe consequences: not only will they distort the peaks' shapes and intensities along the direct and indirect spectral dimensions, but they may also substantially complicate the performance of the water suppression sequence. Indeed, we found that introducing a majority of mixing sequences into the ultrafast 2D experiment resulted in a reappearance of the previously suppressed solvent resonance. This made it difficult to observe the low-abundance metabolites (presumably due to radiation damping effects), and this also led to broader resonances along the direct spectral domains of these acquisitions.

AQ: 7

CONCLUSIONS

The main purpose of the present study was to explore the feasibility of extending ultrafast 2D acquisition protocols that were recently demonstrated on high-resolution NMR hardware to microimaging and animal imaging platforms. We believe that one of the key modifications to make ultrafast 2D spectroscopy feasible in such systems is to replace the currently-implemented square-wave gradients with sinusoidal ones. Applying these (or similarly shaped) gradients allows one to fit dwell times Δt_2 that are suitable for spectroscopic characterizations along the direct dimension, while accommodating a reasonable spectral width (>4 ppm) along k/ν_1. This would simply be unfeasible if the intrinsically long gradient switching times characterizing square-shaped operations (≥200 μs), would have to be inserted in between positive and negative gradients. Despite this advantage, a number of technical obstacles that are not encountered in a standard spectroscopic setting remain to be resolved in the imaging systems, including eddy-driven distortions of the peaks along direct and indirect dimensions, and limitations introduced by the action of the oscillating gradients toward achieving an efficient suppression of the water signal. Also, the peaks' point-spread functions (PSFs) observed for in vivo situations along k/ν_1 may be affected by heterogeneities that are absent in conventional spectroscopic analyses. This feature may actually be exploited to acquire spatially-localized 2D spectral information within a single scan (20). Given additional ongoing improvements in the execution of ultrafast 2D NMR experiments, it is likely that several of these remaining technical obstacles will eventually be overcome, leading to a valuable addition to the current toolbox of MR-based methods for in vivo analysis and diagnosis.

AQ: 8

ACKNOWLEDGMENTS

We thank Mr. Yoav Shrot, Mr. Boaz Shapira, Dr. Adonis Lupulescu, Dr. Tali Scherf, and Dr. Peter Bendel for their assistance during the course of this study.

REFERENCES

1. Burtscher IM, Holtas S. Proton MR spectroscopy in clinical routine. J Magn Reson Imaging 2001;13:560–567.

AQ: 9

2. Burlina AP, Aureli T, Bracco F, Conti F, Battistin L. MR spectroscopy: a powerful tool for investigating brain function neurological diseases. Neurochem Res 2000:1365–1372.
3. Malhi GS, Valenzuela M, Wen W, Sachdev P. Magnetic resonance spectroscopy and its applications in psychiatry. Austral N Z J Psychiatry 2002;36:31–43.
4. Ryner LN, Sorenson JA, Thomas MA. 3D localized 2D NMR spectroscopy on an MRI scanner. J Magn Reson B 1995;107:126–137.
5. Thomas MA, Ryner LN, Mehta MP, Turski PA, Sorenson JA. Localized 2D J-Resolved ^{1}H MR spectroscopy of human brain. J Magn Reson Imaging 1996;6:453–459.
6. Thomas MA, Yue K, Binesh N, Davanzo P, Kumar A, Siegel B, Frye M, Curran J, Lufkin R, Martin P, Guze B. Localized two-dimensional shift correlated MR spectroscopy of human brain. Magn Reson Med 2001; 46:58–67.
7. Ziegler A, Gillet B, Beoeil J, Macher J, Decorps M, Nedelec J. Localized 2D correlation spectroscopy in human brain at 3T. MAGMA 2001;14: 45–49.
8. Watanabe H, Ishihara Y, Okamoto K, Oshio K, Kanamatsu T, Tsukada Y. 3D Localized ^{1}H-^{13}C heteronuclear single-quantum coherence correlation spectroscopy *in vivo*. Magn Reson Med 2000;43:200–210.
9. Von Kienlin M, Ziegler A, Le Fur Y, Rubin C, Decorps M, Remy C. 2D-spatial/2D-spectral spectroscopic imaging of intracerebral gliomas in rat brain. Magn Reson Med 2000;43:211–219.
10. Ke Y, Cohen BM, Bang JY, Yang M, Renshaw PF. Assessment of GABA concentration in human brain using two-dimensional proton magnetic resonance spectroscopy. Psychiatry Res Neuroimaging 2000;100:169–178.
11. Thomas MA, Binesh N, Yue K, DeBruhl N. Volume-localized two-dimensional correlated magnetic resonance spectroscopy of human breast cancer. J Magn Reson Imaging 2001;14:181–186.
12. Yue K, Marumoto A, Binesh N, Thomas MA. 2D JPRESS of human prostates using endorectal receiver coil. Magn Reson Med 2002;47: 1059–1064.
13. Kessler H, Gehrke M, Griesinger C. Two-dimensional NMR spectroscopy: background and overview of the experiments. Angew Chem Int Ed Engl 1988;27:490–536.
14. Freeman R, Kupce E. New methods for fast multidimensional NMR. J Biomolec NMR 2003;27:101–113.
15. Frydman L, Scherf T, Lupulescu A. The acquisition of multidimensional NMR spectra within a single scan. Proc Natl Acad Sci USA 2002;99:15858–15862.
16. Frydman L, Lupulescu A, Scherf T. Principles and features of single-scan two-dimensional NMR spectroscopy. J Am Chem Soc 2003;30: 9204–9217.
17. Shapira B, Lupulescu A, Shrot Y, Frydman L. Line shape considerations in ultrafast 2D NMR. J Magn Reson 2004;166:152–163.
18. Wielopolski PA, Schmitt F, Stehling MK. Echo planar imaging pulse sequences. In: Schmitt F, Stehling MK, Turner R, editors. Echo-planar imaging: theory, technique and application. Berlin/Heidelberg: Springer-Verlag; 1998. p 65–139.
19. Haase A, Frahm J, Hanicke W, Matthei D. Proton NMR chemical shift selective (CHESS) imaging. Phys Med Biol 1985;30:341–344.
20. Shrot Y, Frydman L. Spatially-resolved multidimensional NMR spectroscopy within a single scan. J Magn Reson 2004;167:42–48.

AQ1: Is it OK to add "Theory" head here?

AQ2: Author: Please check the position of the math in the text carefully. In some cases, the position of the math in the digital file did not match the position in the printed manuscript.

AQ3: Is "One can reverse the effective. . ." OK as rewritten?

AQ4: Is "The incorporation of. . ." OK as rewritten?

AQ5: Please define TOCSY.

AQ6: Is "The potential of the current approach" as meant?

AQ7: Is "This drop in quality. . .The decrease in quality was only marginally. . ." OK as rewritten? Please define COSY.

AQ8: Is "We believe that. . ." sentence OK as rewritten?

AQ9: Ref. 2: Please provide volume number.

AQ10: Fig. 4: What is meant instead of "Idem"?